

A CRLB ANALYSIS OF AOA ESTIMATION USING BLUETOOTH 5

Wentao Shi¹²³, Baoqi Huang¹²³ *and Kai Sun⁴

¹Engineering Research Center of Ecological Big Data, Ministry of Education, China

²Inner Mongolia Key Laboratory of Wireless Networking and Mobile Computing

³College of Computer Science, Inner Mongolia University, Hohhot 010021, China

⁴College of Electronic Information Engineering, Inner Mongolia University, Hohhot 010021, China

ABSTRACT

Angle of arrival (AoA) and angle of departure (AoD) are introduced in Bluetooth 5 to better support indoor localization and tracking. However, the performance of AoA estimation using Bluetooth 5 is not thoroughly understood at present. In this paper, a Cramér-Rao lower bound (CRLB) model, taking into account Constant Tone Extension (CTE) signals firstly adopted by Bluetooth 5, is proposed to theoretically analyze its performance given different uniform antenna arrays, such as linear, rectangular and circular arrays, and on these grounds, the effects of the number of antennas, inter antenna distance, incident angle, and CTE parameters on AoA estimation are carefully investigated. A simulation analysis is carried out and a comparison between different types of antenna arrays is reported as well.

Index Terms— Bluetooth 5, AoA estimation, uniform antenna array, CRLB.

1. INTRODUCTION

In recent years, researchers have conducted tremendous research and development of indoor localization based on various wireless technologies [1]-[8]. Among them, indoor localization systems using Bluetooth low energy (BLE) have great advantages on cost, availability, energy efficiency, latency, and scalability, with the exception of accuracy [9]-[14]. Moreover, the Bluetooth Special Interest Group (SIG) announced that the Bluetooth 5.1 specification includes a new “direction finding” function by introducing, Constant Tone Extension (CTE) signals, which significantly improves the localization accuracy to a centimeter level [15]-[16].

Bluetooth 5 has received widespread attention in both industries and academia. In [20], the well-known multiple signal classification (MUSIC) algorithm was applied to implement the AoA estimation based on Bluetooth 5. In [17], the performance of AoA estimation based on Bluetooth 5 has been experimentally studied by using Software Defined Radio (SDR). Although theoretical performance analyses on AoA and AoD estimation have been extensively studied using, e.g. CRLB [18]-[19], none of them take into consideration CTE mechanism adopted by Bluetooth 5. Moreover, the influence of dif-

ferent antenna arrays on AoA estimation using Bluetooth 5 is also unclear.

In order to address this issue, we formulate the CRLBs of AoA estimation by taking into account the parameters specifying the implementation of CTE with respect to three different uniform antenna layouts, i.e. linear, rectangular and circular. On these grounds, the influences of various factors on the performance of AoA estimation using Bluetooth 5 are investigated through both theoretical and simulational perspectives. In addition, three types of antenna arrays are compared.

2. PROBLEM STATEMENT

Taking AoA as an example, as shown in Fig.1, the direction finding signal emitted by a single antenna at a transmitter will arrive at the antennas L_1, L_2, \dots , and L_n in the receiving antenna array at different times due to different transmission distances, resulting a phase difference between any two adjacent antennas (say L_1 and L_2), denoted $\Delta\phi$; given $\Delta\phi$, the inter antenna distance d and the signal wavelength λ , it is evident that the distance b and thus the incident angle, denoted θ , can be inferred as follows [16]

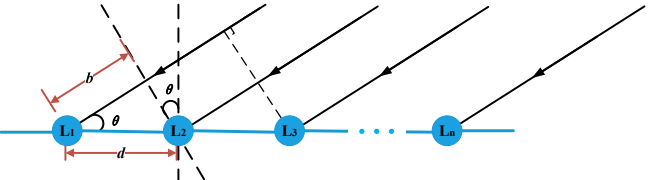
$$\theta = \arccos\left(\frac{b}{d}\right) = \arccos\left(\frac{\lambda\Delta\phi}{2\pi d}\right). \quad (1)$$


Fig. 1. Principle of AoA detection using Bluetooth 5 with a linear antenna array.

However, when more than 2 antennas are available, the problem of estimating θ becomes overdetermined, so that various optimization algorithms can be employed to find a most probable estimate.

BLE devices that support AoA incorporate an additional field called CTE in the physical layer of the LE1M unencoded packet to detect the In-phase (I) and Quadrature (Q) of signals more convenient and accurate, so as to obtain a more reliable $\Delta\phi$. The processing of CTE is divided into an initial guard time of $4\mu s$, a reference time of $8\mu s$, and a subsequent m pairs of switch and sample slots with $m > 1$, as depicted in Fig.2. In each pair of the slots, the receiver will switch to a specific antenna during the corresponding

*Thanks to the National Natural Science Foundation of China (Grant No. 41871363 and 42161070), the Key Science Technology Project of Inner Mongolia Autonomous Region (Grant No. 2021GG0163), and the Major Program of Natural Science Foundation of Inner Mongolia Autonomous Region of China (Grant No. 2021ZD13).

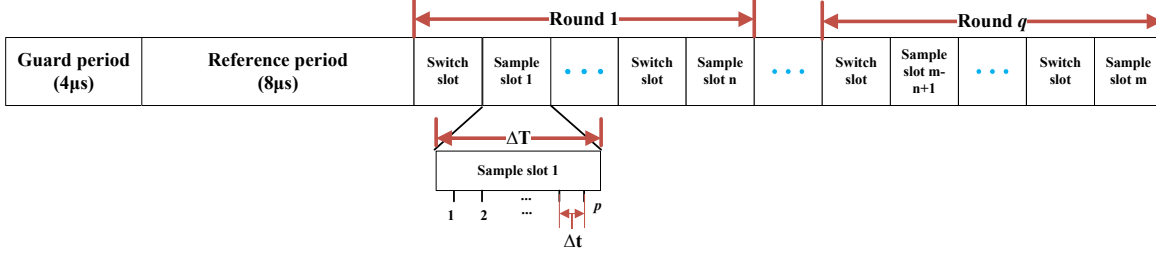


Fig. 2. Illustration of a complete CTE signal.

switch slot and then sample IQ signals at a given sampling rate during the corresponding sample slot. And the IQ samples are generated based on a $f_c=2.402\sim 2.480$ GHz BLE signal plus a $f_d = 250$ KHz GFSK frequency shift. The length of CTE is at most $160 \mu s$ according to the configuration of m , and since the duration of each slot is either $1 \mu s$ or $2 \mu s$, there will be at most 37 or 74 pairs of switch and sample slots in one CTE.

Consider a far-field transmitter with a single antenna in a 2-D plane continuously transmitting Bluetooth 5 signals to a receiver with n dipole antennas. As shown in Fig.2, the receiver configures each antenna to sample p times in each sample slot. Provided that the duration of each slot is $\Delta T \mu s$, the interval between two adjacent sampling times in a sample slot is $\Delta t \mu s$ ($\Delta t = \frac{\Delta T}{p}$). When n antenna are sampled during n continuous pairs of slots, it is called a sampling round. Without loss of generality, and let each antenna be sampled by the same times, denoted q , namely that $q = \frac{m}{n}$. Besides, define ϕ_{ijk}^S to be the ground-truth phase value corresponding to the j th sampling of i th antenna in the k th sampling round, where the superscript S takes value from $\{L, R, C\}$ (standing for the uniform linear, rectangular and circular antenna layouts) $i = 1, \dots, n$, $j = 1, \dots, p$ and $k = 1, \dots, q$; and let $\tilde{\phi}_{ijk}^S$ be the corresponding phase measurement suffering white Gaussian noises with the standard deviation of σ . In addition, define c to be the signal speed.

3. THEORETICAL ANALYSIS

In this section, we formulate the CRLBs of AoA estimation using Bluetooth 5 with respect to different uniform antenna layouts, and then provide corresponding theoretical analyses.

3.1. Uniform linear array

Definition 1: A uniform linear array (ULA) is defined as arranging n ($n > 2$) identical dipole antennas built in a receiver, i.e. L_1, L_2, \dots , and L_n , in a linear style with the space of d , as shown in Fig.1.

Suppose that a far-field signal is emitted by a transmitter and arrives at the receiver with the incident angle θ . Without loss of generality, let the antenna L_1 be the reference antenna, in the sense that the ground-truth phase value obtained through L_1 in the first time is ϕ_0^L . According to the distance difference and sampling time delay incurred by different antennas, we can have

$$\phi_{ijk}^L = \left[\phi_0^L + 2(j-1)\pi f_d \Delta t + 4(i-1)\pi f_d \Delta T + 4(k-1)n\pi f_d \Delta T + \frac{2(i-1)\pi f_c d \cos \theta}{c} \right] (\text{mod } 2\pi), \quad (2)$$

Therein, the term $2(j-1)\pi f_d \Delta t$ reflects the phase change caused by the time delay of different sampling instances in one sam-

pling slot, the term $4(i-1)\pi f_d \Delta T$ reflects the phase change caused by switching to different antennas, the term $4(k-1)n\pi f_d \Delta T$ reflects the phase change caused by different sampling rounds, the term $2(i-1)\pi f_c d \cos \theta / c$ reflects the phase change caused by the incident angle as well as the distance difference among different antennas, and the modular operation is applied to restrict the phase value fall in $[0, 2\pi)$. Because we found that the phase value of the signal in actual measurement is obtained by the atan2 function in the range of phase $(-\pi, \pi]$, we can map the result of the function to the range $[0, 2\pi)$ by adding 2π on the negative result.

According to the assumption on white Gaussian noises in phase measurements, we have $\tilde{\phi}_{ijk}^L \sim N(\phi_{ijk}^L, \sigma^2)$ with the result that the likelihood function corresponding to the AoA estimation, namely the estimation of θ , can be obtained as follows

$$\begin{aligned} \ell(\tilde{\phi}_{ijk}^L; \theta) &= \log \prod_{i=1}^n \prod_{j=1}^p \prod_{k=1}^q p(\tilde{\phi}_{ijk}^L) \\ &= \sum_{i=1}^n \sum_{j=1}^p \sum_{k=1}^q \log p(\tilde{\phi}_{ijk}^L) \\ &= \sum_{i=1}^n \sum_{j=1}^p \sum_{k=1}^q \log \left[\frac{1}{\sqrt{2\pi}\sigma} \exp \left(-\frac{(\tilde{\phi}_{ijk}^L - \phi_{ijk}^L)^2}{2\sigma^2} \right) \right]. \end{aligned} \quad (3)$$

The corresponding Fisher information matrix (FIM) can be obtained as follows

$$F_L(\theta) = \frac{2n(n-1)(2n-1)pmf_c^2 d^2 \pi^2 \sin^2 \theta}{3\sigma^2 c^2}. \quad (4)$$

Finally, with the ULA, we can derive the CRLB of the AoA estimation problem as follows

$$F_L^{-1}(\theta) = \frac{3\sigma^2 c^2}{2n(n-1)(2n-1)pmf_c^2 d^2 \pi^2 \sin^2 \theta}. \quad (5)$$

3.2. Uniform rectangular array

Definition 2: A uniform rectangular array (URA) is defined as arranging an even number of n (n is even and ≥ 4) identical dipole antennas built in a receiver, i.e. R_1, R_2, \dots , and R_n , in a rectangular style with the space of d , as shown in Fig.4.

Consider the same situation as the ULA and let the antenna R_1 be the reference antenna. When $i \in [1, \frac{n}{2}]$, the phase value is calculated as in the ULA case, namely

$$\begin{aligned} \phi_{ijk}^R &= [2(j-1)\pi f_d \Delta t + 4(i-1)\pi f_d \Delta T + 4(k-1)n\pi f_d \Delta T \\ &\quad + \phi_0^R + \frac{2(i-1)\pi f_c d \cos \theta}{c}] (\text{mod } 2\pi). \end{aligned} \quad (6)$$

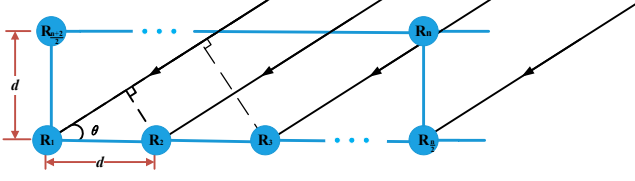


Fig. 3. Example floor plan for URA.

But, when $i \in [\frac{n+2}{2}, n]$, the geometry between the i th antenna and the reference antenna becomes different, and thus, we can have

$$\phi_{ijk}^R = \left\{ 2(j-1)\pi f_d \Delta t + 4(i-1)\pi f_d \Delta T + 4(k-1)n\pi f_d \Delta T + \phi_0^R + \frac{2\pi f_c d}{c} \left[\left(\frac{2i-(n+2)}{2} \right) \cos \theta + \sin \theta \right] \right\} \pmod{2\pi}. \quad (7)$$

Therein, the term $\frac{2\pi f_c d}{c} \left[\left(\frac{2i-(n+2)}{2} \right) \cos \theta + \sin \theta \right]$ reflects the phase change caused by the incident angle θ as well as the distance difference among different antennas in equation (7).

Similar with the ULA case, we can derive the CRLB of the AoA estimation problem in the URA case as follows

$$F_R^{-1}(\theta) = \frac{\sigma^2 c^2}{4pmf_c^2 d^2 \pi^2} \left[\left(\frac{3n^4 - 4n^3 - 12n^2 + 16n}{24} \right) \sin^2 \theta - \left(\frac{n^3 - 4n}{2} \right) \sin \theta \cos \theta + 2n \cos^2 \theta \right]^{-1}. \quad (8)$$

3.3. Uniform circular array

Definition 3: A uniform circular array (UCA) is defined as arranging n ($n \geq 3$) identical dipole antennas built in a receiver, i.e. C_1, C_2, \dots , and C_n , in a circular style with the radius of r as shown in Fig.4.

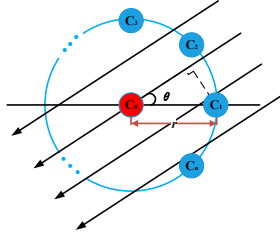


Fig. 4. Example floor plan for UCA.

For ease of calculations, we introduce a virtual antenna placed at the center of UCA, denoted C_0 , and let C_0 be the reference antenna. Moreover, without loss of generality, suppose that C_1 is located at the horizontal axis. Then, we can obtain

$$\phi_{ijk}^C = \left[(j-1) \cdot 2\pi \Delta t f_d + (i-1) \cdot 4\pi \Delta T f_d + 4(k-1)n\pi f_d \Delta T + \phi_0^C + \frac{2\pi r f_c}{c} \cos \left(\frac{2\pi(i-1)}{n} - \theta \right) \right] \pmod{2\pi}, \quad (9)$$

where the term $\frac{2\pi r f_c}{c} \cos \left(\frac{2\pi(i-1)}{n} - \theta \right)$ reflects the phase change caused by the incident angle as well as the distance difference among different antennas.

Similarly, with the UCA, we can derive the CRLB of the AoA estimation problem as follows

$$F_C^{-1}(\theta) = \frac{\sigma^2 c^2}{4pmf_c^2 r^2 \pi^2 \sum_{i=1}^n \sin^2 \left[\theta - \frac{2\pi(i-1)}{n} \right]}. \quad (10)$$

After substitute r by the expression involving the antenna distance d , we can have

$$F_C^{-1}(\theta) = \frac{\sigma^2 c^2 \sin^2 \left(\frac{\pi}{n} \right)}{pmf_c^2 d^2 \pi^2 \sum_{i=1}^n \sin^2 \left[\theta - \frac{2\pi(i-1)}{n} \right]}. \quad (11)$$

3.4. The RMSE of AoA estimation and analysis

In order to intuitively analyze the influence of each parameter in the formulae on the AoA estimation, the root mean squared error (RMSE) of AoA is evaluated as follows

$$\text{RMSE}_L = \sqrt{F_L^{-1}(\theta)} = \sqrt{\frac{3}{2pmn(n-1)(2n-1)} \frac{\sigma c}{\pi d f_c \sin \theta}}, \quad (12)$$

$$\begin{aligned} \text{RMSE}_R &= \sqrt{F_R^{-1}(\theta)} \\ &= \frac{\sigma c}{2\pi d f_c \sqrt{pm}} \left[\left(\frac{3n^4 - 4n^3 - 12n^2 + 16n}{24} \right) \sin^2 \theta - \left(\frac{n^3 - 4n}{2} \right) \sin \theta \cos \theta + 2n \cos^2 \theta \right]^{-\frac{1}{2}}, \quad (13) \end{aligned}$$

$$\text{RMSE}_C = \sqrt{F_C^{-1}(\theta)} = \frac{\sigma c \sin \left(\frac{\pi}{n} \right)}{\pi f_c d \sqrt{pm \sum_{i=1}^n \sin^2 \left[\theta - \frac{2\pi(i-1)}{n} \right]}}. \quad (14)$$

According to the RMSEs in (12), (13) and (14), the following conclusions can be drawn:

- 1) It is evident that, in all the three cases, the RMSEs are proportional to the phase measurement noise level (i.e. σ), and are inversely proportional to the antenna distance d and the signal frequency f_c . In particular, the performance of the AoA estimation improves with the increase of the antenna distance d , which cannot exceed a half of the signal wavelength, e.g. 0.625m for Bluetooth 5.
- 2) The RMSE in the ULA case reduces with the number of antennas (i.e. n) increasing and periodically varies with the incident angle θ , but the relationships between the RMSE and n and θ in the URA and UCA cases are implicit, and will be investigated through simulations in the following section.
- 3) Regarding the configuration parameters of CTE signals, i.e. p and m , it is intuitive that the RMSEs in all the three cases decrease with increasing p and m , which is attributable to the fact that more information is acquired for AoA estimation.

4. SIMULATION ANALYSIS

In this section, we shall conduct a simulation analysis to further investigate how the performance of AoA estimation using Bluetooth 5 is affected.

4.1. The influences of the antenna array parameters

The main parameters of an antenna array include the antenna distance d and the number of antennas n . According to the previous analysis in section 3, the antenna distance is inversely proportional to the RMSEs of AoA estimation of three antenna array layouts. To explore in detail the trend of RMSE with the antenna distance, we consider two representative cases (i.e. $n=8$, $\theta=45^\circ$ and $n=12$, $\theta=90^\circ$) while keeping other parameters default (i.e. $p=1$, $m=37$ and $\sigma=2$). As shown in Fig.5(a), the performance of AoA estimation in the UCA case is more sensitive to changes in the antenna distance d , and it is basically the same in the ULA and URA cases. When the number of antennas n is large and the incident angle θ is closer to 90° , the influence of antenna distance on the performance of AoA estimation will become weaker.

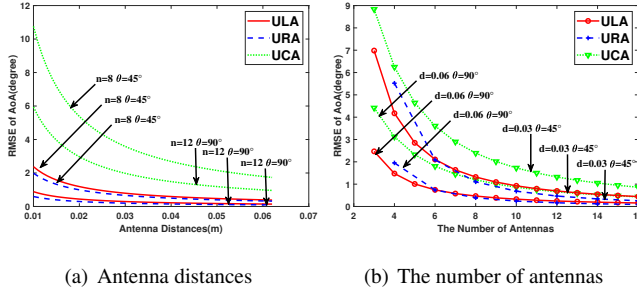


Fig. 5. The RMSE of AoA estimation given different antenna array parameters.

In order to obtain the influence of the number of antennas on the performance of AoA estimation in all the three cases, this paper carried out simulations under the two conditions ($d=0.03$, $\theta=45^\circ$ and $d=0.06$, $\theta=90^\circ$) with the other signal parameters default (i.e. $p=1$, $m=37$ and $\sigma=2$). It can be observed that the performance of AoA estimation of three uniform antenna arrays reduce with the increase of the number of antennas in Fig.5(b). What's more, when the antenna distance d and the incident angle θ are in the proper range, the number of antennas in the ULA and URA cases are needed to be set to 8, and the number of antennas in the UCA case to 10, in order to obtain a better AoA estimation performance. If we continue to increase the number of antennas, it will be of little significance to improve the AoA estimation performance.

4.2. The influences of CTE parameters

Our simulation results have shown that the AoA estimation performance of ULA is extremely poor when the incident angle θ is close to 0 and π . This phenomenon has been observed in some existing AoA estimation work [21]-[22]. To explore the influence of the incident angle, this paper simulates under two conditions ($n=8$, $d=0.03$ and $n=12$, $d=0.06$) with the other parameters default (i.e. $p=1$, $m=37$ and $\sigma=2$) and discards the display of partial angle range results in Fig.6(a). We find that the AoA estimation performance of UCA is not affected by changes in the incident angle θ because of the radial symmetry. At the same time, when the antenna distance d and the number of antennas n are large enough, the impact of the incident angle θ on the AoA estimation performance of ULA and URA performance will be greatly reduced, even reaching an effect similar to UCA.

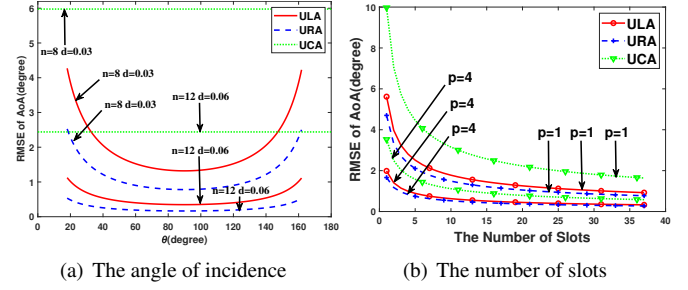


Fig. 6. The RMSE of AoA estimation given different CTE signal parameters

The researchers usually set the CTE signal length to $160 \mu s$ to obtain a great AoA estimation. However, this paper simulates the number of slots and acquisition frequency (i.e. $p=1$ and $p=4$) when the antenna array parameters and the signal incident angle are exactly the same (i.e. $n=8$, $d=0.03$, $\sigma=2$ and $\theta=60^\circ$). According to Fig.6(b) shows that when the number of Sample slots reaches 20, the AoA estimation performance of three uniform antenna arrays will hardly improve. On the other hand, if the length of CTE signal is long enough, that is, with more than 15 Sample slots, the acquisition frequency will have little effect on the AoA estimation performance.

4.3. Some suggestions

Based on these theoretical and simulation analyses, this paper have carried out useful opinions for practical work.

- 1) The antenna distances of ULA and URA should be controlled above 0.03m, and the antenna distance of UCA should be set above 0.04m. Especially, the antenna distance has a great influence on the AoA estimation performance of UCA.
- 2) When the above antenna distances design requirements are met, no matter which uniform antenna array is used, the number of antennas should be set to 8 at least. At this time, a better AoA estimation result can be achieved, and the antenna array cost can be reduced as much as possible. When the number of antennas is $8 \sim 16$, the AoA estimation performance of URA is the best in the proper incident angle range. When the number of antennas is 16 or more, the AoA estimation of UCA is the best at each incident angle.
- 3) No matter what the length of slot and acquisition frequency are used, as long as the number of slots of a CTE signal reaches 15, it is possible to achieve better AoA estimation performance in each antenna layout.

5. CONCLUSION

In this paper, we used CRLB to investigate how the factors that affect the AoA estimation under various conditions based on Bluetooth 5. Through a theoretical analysis, the key factors of influencing indoor localization accuracy based on Bluetooth 5 were obtained. What's more, this paper laid a solid foundation for future studies on AoA estimation in complex situations, such as non-uniform antenna arrays and multiple transmitters.

6. REFERENCES

- [1] F. Zafari, A. Gkelias, and K. K. Leung, "A survey of indoor localization systems and technologies," *IEEE Commun. Surveys Tuts.*, vol. 21, no. 3, pp. 2568–2599, 3rd Quart, 2019.
- [2] Y. Li, Z. He, Z. Gao, Y. Zhuang, C. Shi, and N. El-Sheimy, "Toward robust crowdsourcing-based localization: A fingerprinting accuracy indicator enhanced wireless/magnetic/inertial integration approach," *IEEE Internet of Things Journal*, vol. 6, no. 2, pp. 3585–3600, Apr. 2019.
- [3] B. Huang, Z. Xu, B. Jia And G. Mao, "An Online Radio Map Update Scheme For WiFi Fingerprint-Based Localization," *IEEE Internet Of Things Journal*, Vol.6, no.4, pp.6909-6918, Aug. 2019.
- [4] H. Tian and L. Zhu, "MIMO CSI-based Super-resolution AoA Estimation for Wi-Fi Indoor Localization," in *2020 ICTCE 12th International Conference on Machine Learning and Computing*, Feb. 2020, pp. 457–461.
- [5] D. Feng, C. Wang, C. He, Y. Zhuang, and X. Xia, "Kalman-filter-based integration of IMU and UWB for high-accuracy indoor positioning and navigation," *IEEE Internet of Things Journal*, vol. 7, no. 4, pp. 3133–3146, Apr. 2020.
- [6] B. Huang, L. Xie, Z. Yang, "TDOA-Based Source Localization With Distance-Dependent Noises," *IEEE Transactions On Wireless Communications*, Vol.14, no.1, pp.468-480, Jan. 2015.
- [7] G. Avitabile, A. Florio and G. Coviello, "Angle of Arrival Estimation Through a Full-Hardware Approach for Adaptive Beamforming," *IEEE Transactions on Circuits and Systems II: Express Briefs*, vol. 67, no. 12, pp. 3033-3037, Dec. 2020.
- [8] Y. Zhuang, Q. Wang, M. Shi, P. Cao, L. Qi, and J. Yang, "Low-power centimeter-level localization for indoor mobile robots based on ensemble Kalman smoother using received signal strength," *IEEE Internet of Things Journal*, vol. 6, no. 4, pp. 6513–6522, Aug. 2019.
- [9] Y. Tian, B. Huang, B. Jia And L. Zhao, "Optimizing AP And Beacon Placement In WiFi And BLE Hybrid Localization," *Journal Of Network And Computer Applications*, Vol. 164, No. 102673, pp. 1-11, 2020.
- [10] S. Bertuletti, A. Cereatti, M. Caldara, M. Galizzi and U. Della Croce, "Indoor distance estimated from Bluetooth Low Energy signal strength: Comparison of regression models," in *2016 IEEE Sensors Applications Symposium (SAS)*, Catania, 2016, pp. 1-5.
- [11] J. Larsson, "Distance Estimation and Positioning Based on Bluetooth Low Energy Technology," Kista, 2015.
- [12] W. He, P. Ho, and J. Tapolcai, "Beacon deployment for unambiguous positioning," *IEEE Internet of Things Journal*, vol. 4, no. 5, pp. 1370–1379, Oct. 2017.
- [13] C. Huang, H. Liu, W. Wang, and J. Li, "A compact and cost-effective BLE beacon with multiprotocol and dynamic content advertising for IoT application," *IEEE Internet of Things Journal*, vol. 7, no. 3, pp. 2309–2320, Mar. 2020.
- [14] M. Cominelli, P. Patras, and F. Gringoli, "Dead on arrival: An empirical study of the Bluetooth 5.1 positioning system," in *Proceedings of the 13th International Workshop on Wireless Network Testbeds, Experimental Evaluation & Characterization*, 2019, pp. 13-20.
- [15] M. Woolley. (Mar. 2019). *Bluetooth Direction Finding: A Technical Overview*. [Online]. Available: <https://www.bluetooth.com/bluetoothresources/bluetooth-direction-finding/>.
- [16] M. Woolley. (Jan. 2019). *Bluetooth Core Specification V5.1 Feature Overview*. [Online]. Available: <https://www.bluetooth.com/bluetoothresources/bluetooth-core-specification-v5-1-feature-overview/>.
- [17] F. A. Toasa, L. Tello-Oquendo, C. R. Peñafiel-Ojeda and G. Cuzco, "Experimental Demonstration for Indoor Localization Based on AoA of Bluetooth 5.1 Using Software Defined Radio," in *2021 IEEE 18th Annual Consumer Communications Networking Conference (CCNC)*, 2021, pp. 1-4.
- [18] Z. Liu, "Conditional Cramér–Rao Lower Bounds for DOA Estimation and Array Calibration," *IEEE Signal Processing Letters*, vol. 21, no. 3, pp. 361-364, Mar. 2014.
- [19] J. Xu, M. Ma, and C. L. Law, "AoA cooperative position localization," in *IEEE GLOBECOM 2008 - 2008 IEEE Global Telecommunications Conference*, Nov. 2008, pp. 1–5.
- [20] S. Monfared, T. Nguyen, L. Petrillo, P. De Doncker and F. Horlin, "Experimental Demonstration of BLE Transmitter Positioning Based on AOA Estimation," in *2018 IEEE 29th Annual International Symposium on Personal, Indoor and Mobile Radio Communications (PIMRC)*, 2018, pp. 856-859.
- [21] I. Kadar, "Optimum geometry selection for sensor fusion," *Signal Processing, Sensor Fusion, and Target Recognition VII*, 1998, pp. 96–107.
- [22] F. Bellili, A. Methenni and S. Affes, "Closed-Form CRLBs for CFO and Phase Estimation From Turbo-Coded Square-QAM-Modulated Transmissions," *IEEE Transactions on Wireless Communications*, vol. 14, no. 5, pp. 2513-2531, May. 2015.
- [23] A. N. Bishop, B. Fidan, B. D. O. Anderson, K. Doğançay and P. N. Pathirana, "Optimality analysis of sensor-target localization geometries," *Automatica*, 2010, 46(3): 479-492.
- [24] C. Li, T. Jens, P. David, T. Emmeric, H. Jeroen, P. D. Eli, and J. Wout, "CRLB-based Positioning Performance of Indoor Hybrid AoA/RSS/ToF Localization," in *2019 International Conference on Indoor Positioning and Indoor Navigation (IPIN)*, Pisa, Italy, 2019, pp. 1-6.
- [25] J. Shim, H. Park, C. Chae, D. K. Kim and Y. C. Eldar, "Cramér–Rao Lower Bound on AoA Estimation Using an RF Lens-Embedded Antenna Array," *IEEE Antennas and Wireless Propagation Letters*, vol. 17, no. 12, pp. 2359-2363, Dec. 2018.